Research Square

Preprints are preliminary reports that have not undergone peer review.
They should not be considered conclusive, used to inform clinical practice,
or referenced by the media as validated information.

# Transcriptome and proteome analyses reveal high nitrate or ammonium applications alleviate photosynthetic decline of Phoebe bournei seedlings under elevated carbon dioxide by regulating glnA and rbcS

**Xiao Wang**
Guizhou University
**Xiaoli Wei**
gdwxl-69@126.com
Guizhou University
**Gaoyin Wu**
Guizhou University
**Shengqun Chen**
Guizhou University

**Research Article**

**Keywords:** Phoebe bournei, Carbon dioxide, Nitrogen,Transcriptomic, Proteomic

**Posted Date:** August 1st, 2022

**DOI:** https://doi.org/10.21203/rs.3.rs-1861132/v1

**License:** This work is licensed under a Creative Commons Attribution 4.0 International License. Read Full License

**Additional Declarations:** No competing interests reported.

**Version of Record:** A version of this preprint was published at Physiology and Molecular Biology of Plants on July 18th, 2024. See the published version at https://doi.org/10.1007/s12298-024-01481-2.

## Abstract

# Background

*Phoebe bournei* (Hemsl.) Y.C. Yang is a precious timber species and is listed as a national secondary protection plant in China. *P. bournei* seedlings show obvious photosynthetic decline when grown long-term under an elevated $CO_2$ concentration ($eCO_2$). This decline can be alleviated by high nitrate or ammonium applications. However, the underlying mechanisms of photosynthetic decline and the regulation of photosynthesis by nitrogen under $eCO_2$ have not yet been elucidated.

# Results

We performed transcriptomic and proteomic analyses of *P. bournei* of seedlings grown under an ambient $CO_2$ (AC) concentration (350 ± 70μmol·mol$^{-1}$) and applied with either a moderate level of nitrate(0.8 g per seedling, N), a high level of nitrate (1.2 g per seedling, hN), or a moderate level of ammonium (0.8 g per seedling, A) and compared them with those of seedlings grown under an elevated $CO_2$ (EC) concentration (700 ± 10μmol·mol$^{-1}$,i.e., AC_N vs EC_N, AC_hN vs EC_hN, AC_A vs EC_A) to identify differentially expressed genes (DEGs) and differentially expressed genes (DEGs). We identified 4528 (AC_N vs EC_N), 1378 (AC_hN vs EC_hN), and 252 (AC_A vs EC_A) DEGs and 230, 514, and 234 DEPs, respectively, of which 59 specific genes and 21 specific proteins were related to the regulation of photosynthesis by nitrogen under $eCO_2$. A combined transcriptomic and proteomic analysis identified 7 correlation-DEGs-DEPs (cor-DEGs-DEPs) genes. Kyoto Encyclopedia of Genes and Genomes (KEGG) enrichment analyses of these cor-DEGs-DEPs genes revealed crucial pathways involved in glyoxylate and dicarboxylate metabolism and nitrogen metabolism. The *rbcS* and *glnA* cor-DEGs-DEPs genes were enriched in these two metabolisms. We propose that the *rbcS* and *glnA* cor-DEGs-DEPs genes play an important role in photosynthetic decline and nitrogen regulation.

# Conclusions

Transcriptomic and proteomic profiles of *P. bournei* were used to evaluate elevated $CO_2$ effects on photosynthesis and nitrogen regulation. The elevated $CO_2$ triggered the downregulation of *glnA* and *RbcS*, thus causing photosynthetic decline. High nitrate or ammonium applications alleviated the downregulation of *glnA* and *rbcS* and, hence, alleviated photosynthetic decline.

## Background

Elevated $CO_2$ ($eCO_2$) concentrations have an important effect on plant photosynthesis [1]. Studies had shown that in the short-term, an increase in $CO_2$ concentration increases photosynthetic efficiency; however, in the long-term, photosynthetic efficiency decreases [2–4]. Possible explanations for a photosynthetic decline under long-term $eCO_2$ conditions include an excessive accumulation of carbohydrates [5], inhibition of nitrogen absorption [6], and destruction of the source–sink balance [7].

*Phoebe bournei* (Hemsl.) Y.C. Yang is a precious timber species and is listed as a national secondary protection plant in China. The stem of *P. Bournei* is straight and its wood is dense, tough and fragrant. It is economically important species for building and high-grade furniture. *P. bournei* seedlings show obvious photosynthetic decline when grown long-term under $eCO_2$ [8, 9]. In our previous study [10], we showed that this decline could be alleviated by applying a high level of nitrate or ammonium and that the content of ribulose-1,5-bisphosphate carboxylase/oxygenase (Rubisco) and Rubisco activase (RCA) changed under different $CO_2$ concentrations and nitrogen supplies. We hypothesize that the application of high nitrate or ammonium regulates photosynthetic efficiency by affecting the content of Rubisco and RCA, while the change in the Rubisco and RCA content may reflect a difference in the nitrogen metabolism in *P. bournei* seedlings [11]. The positive effect of $eCO_2$ on wheat production can be maintained by increasing the dose of N fertilizer application [12]. Plants receiving ammonium respond more positively to $eCO_2$ than those receiving nitrate because $eCO_2$ inhibited the assimilation of nitrate in shoots of $C_3$ plants [13]. These findings are consistent with ours; however, the mechanisms underlying photosynthetic decline, especially the regulation of nitrogen remain poorly understood [10]. In this study, our aim was to further elucidate the mechanism involved in the alleviation of the photosynthetic decline of *P. bournei* seedlings under $eCO_2$ when applied with high nitrate or ammonium applications.

With the development of molecular biology technology, transcriptomics and proteomics technologies are providing new ways of identifying target genes and proteins for research studies [14]. Transcriptomic and proteomic analyses have been extensively applied to many plant species [15, 16]. Differential gene expression analysis of *Jatropha curcas* grown under ambient $CO_2$ (~ 0.375 mg·g$^{-1}$) or elevated $CO_2$ (~ 0.550 mg·g$^{-1}$) revealed 3013 transcripts differentially regulated under $eCO_2$ conditions [17]. Transcriptomic changes, including transcripts involved with the tricarboxylic acid cycle [18] and starch and sucrose synthesis [19], that were induced by $eCO_2$ have been found. Proteomic studies had shown changes in the contents of ATP synthase, phosphoglycerate mutase [20], phospho-glycerate kinase and glyceraldehyde-3-phosphate dehydrogenase in plants growing under $eCO_2$ [21]. Proteomic and transcriptomic profile analyses have also revealed that photosynthesis was promoted by regulating *RbcS* and *Rca* when *Vitis vinifera* plantlets are grown under an $eCO_2$ concentration [22]. To understand the mechanism involved in the alleviation of the photosynthetic decline of *P. bournei* seedlings under $eCO_2$ when applied with high nitrate or ammonium, we conducted a comprehensive analysis of the transcriptome and proteome to improve our overall understanding of the potential molecular mechanisms involved.

## Results

### Statistical analysis of differentially expressed transcripts/proteins

The number of DEGs obtained for AC_N vs EC_N, AC_hN vs EC_hN and AC_A vs EC_A was 4528 (3029 were downregulated), 1378 (993 were downregulated), and 252 (16 were downregulated), respectively (Fig. 1a). The number of DEPs obtained for AC_N vs EC_N, AC_hN vs EC_hN and AC_A vs EC_A was 230 (154 were downregulated), 514 (105 were downregulated), and 234 (44 were downregulated), respectively (Fig. 1b).

### GO analysis of DEGs and DEPS

Gene Ontology (GO) analysis indicated that DEGs identified in three comparisons were enriched in the biological process (BP), cellular component (CC), and molecular function (MF) categories. The top 20 categories enriched by DEGs with the most significant *p* values are shown in Additional file 1: Figure S1. In the AC_N vs EC_N comparison, most DEGs in the MF category were involved in small molecule binding, nucleoside phosphate binding, and nucleotide binding, and most DEGs in the CC category were involved in integral components of the membrane, intrinsic components of the membrane, and membrane parts (Additional file 1: Figure S1A). In the AC_hN vs EC_hN comparison, most DEGs in the BP category were involved in the cellular carbohydrate metabolic process or the cellular glucan metabolic process and in kinase activity or protein kinase activity in the MF category (Additional file 1: Figure S1B). In the AC_A vs EC_A comparison, most DEGs in the MF category were involved in nucleic acid binding transcription factor activity, transcription factor activity, or sequence-specific DNA binding and in the response to abiotic stimulus or the cellular response to heat in the BP category (Additional file 1: Figure S1C).

The top 20 categories enriched by DEPs in each of the comparisons with the most significant *p* values are shown in Additional file 2: Figure S2. In the AC_N vs EC_N comparison, most DEPs in the BP category were involved in the regulation of a cellular metabolic process, regulation of a metabolic process, or regulation of a primary metabolic process. Most DEPs in the MF category were involved in GTPase activity, protein tag, or nucleic acid binding (Additional file 2: Figure S2A). In the AC_hN vs EC_hN comparison, most DEPs in the BP category were involved in ribonucleoprotein complex subunit organization, the alcohol metabolic process, or ribonucleoprotein complex assembly and most of those in the MF category were involved in ammonia ligase activity or glutamate-ammonia ligase (Additional file 2: Figure S2B). In the AC_A vs EC_A comparison, 234 DEPs were involved in either transporter activity or transmembrane transporter activity in the MF category or an integral component of the membrane or an intrinsic component of the membrane in the CC category (Additional file 2: Figure S2C).

### KEGG pathway analysis of DEGs and DEPS

DEGs were identified by searching the KEGG database. The 4528 DEGs detected in the AC_N vs EC_N comparison were significantly assigned to 20 KEGG pathways: the top five pathways with the most significant *p* values were plant–pathogen interaction, photosynthesis-antenna proteins, phenylpropanoid biosynthesis, photosynthesis, and isoquinoline alkaloid biosynthesis (Additional file 3: Table S1). The 1378 DEGs detected in the AC_hN vs EC_hN comparison were significantly assigned to 11 KEGG pathways: the top five pathways with the most significant *p* values were plant hormone signal transduction, MAPK signaling pathway – plant, porphyrin and chlorophyll metabolism, phenylalanine, tyrosine and tryptophan biosynthesis and circadian rhythm – plant (Additional file 3: Table S1). The 252 DEGs detected in the AC_A vs EC_A comparison were significantly assigned to three KEGG pathways: protein processing in the endoplasmic reticulum, circadian rhythm – plant and endocytosis (Additional file 3: Table S1).

DEPs were identified by searching the KEGG database. The 230 DEPs detected in the AC_N vs EC_N comparison were significantly assigned to nine KEGG pathways: the top five pathways with the mostsignificant *p* values were glyoxylate and dicarboxylate metabolism, peroxisome, alanine, aspartate and glutamate metabolism, glycine, serine and threonine metabolism, and SNARE interactions in vesicular transport (Additional file 4: Table S2). The 514 DEPs detected in the AC_hN vs EC_hN comparison were significantly assigned to eight KEGG pathways: the top five pathways with the most significant *p* values were phosphatidylinositol signaling system, ubiquinone and other terpenoid-quinone biosynthesis, carotenoid biosynthesis, protein export, and porphyrin and chlorophyll metabolism (Additional file 4: Table S2). The 234 DEPs detected in the AC_A vs EC_A comparison were significantly assigned to four KEGG pathways: ribosome, cutin, suberin and wax biosynthesis, limonene and pinene degradation, and ABC transporters (Additional file 4: Table S2).

### KEGG pathway and cluster analysis of DEGs and DEPs affected by $eCO_2$ and nitrogen supply

From the KEGG pathway analysis, 59 DEGs in the AC_N vs EC_N comparison (53 were downregulated, 6 were upregulated) were significantly assigned to photosynthesis-antenna proteins, photosynthesis, galactose metabolism, nitrogen metabolism, and glyoxylate and dicarboxylate metabolism (Additional file 3: Table S1, Table 1). Six of the downregulated DEGs in the AC_N vs EC_N comparison were not significantly changed in the AC_hN vs EC_hN comparison, 9 out of the 53 downregulated DEGs in the AC_N vs EC_N comparison were upregulated and 44 were not significantly different to those identified in the AC_hN vs EC_hN comparison (Table 2). None of these 59 DEGs in the AC_N vs EC_N comparison showed significantly different expression in the AC_A vs EC_A comparison (Table 2). Therefore, we suggestted that these 59 genes play an important role in the nitrogen regulation of the photosynthetic response to $eCO_2$ in *P. bournei* seedlings. A cluster analysis of expression patterns in the associated DEGs are shown in Additional file 5: Fig. S3.

Twenty-one DEPs in the AC_N vs EC_N comparison (16 were downregulated and 5 were upregulated) were significantly assigned to photosynthesis, glyoxylate and dicarboxylate metabolism (Additional file 4: Table S2, Table 3). Four of the 16 downregulated DEPs in the AC_N vs EC_N comparison were upregulated and 12 were not significantly changed in the AC_hN vs EC_hN comparison (Table 2). None of the 16 downregulated DEPs in the AC_N vs EC_N comparison were significantly changed in the AC_A vs EC_A comparison (Table 2). Hence, we considered that these 21 proteins play an important role in the nitrogen regulation of the photosynthesis response to $eCO_2$ in *P. bournei* seedlings. A cluster analysis of the expression patterns of the associated DEPs are shown in Additional file 6: Fig. S4.

### Comparison of transcriptomic and proteomic data

### Number of DEGs correlated with DEPs

Thirteen, 8, and 5 of the DEPs obtained in the AC_N vs EC_N, AC_hN vs EC_hN, and AC_A vs EC_A comparisons, respectively, were correlated with the corresponding DEGs (Fig. 1). Among the correlation-DEGs-DEPs (cor-DEGs-DEPs) genes, 7 (AC_N vs EC_N), 6 (AC_hN vs EC_hN), and 3 (AC_A vs EC_A) genes showed the same trend, while 6 (AC_N vs EC_N), 2 (AC_N vs EC_N) and 3 (AC_A vs EC_A) genes showed the opposite trend (Fig. 2).

Of the 7 cor-DEGs-DEPs genes in the AC_N vs EC_N comparison, 6 were downregulated and 1 was upregulated. Seven cor-DEGs-DEPs genes in the AC_hN vs EC_hN and AC_A vs EC_A comparison either showed no significant difference in expression or showed the opposite expression to those in the AC_N vs EC_N comparison (Table 3). Thus, we suggest that some of these seven cor-DEGs-DEPs genes might play important roles in alleviating the photosynthetic decline of *P. bournei* under different nitrogen applications.

### Pathway enrichment analysis of cor-DEGs-DEPs genes

KEGG pathway analysis can help to further understand the biochemical metabolic pathways and signal transduction pathways involved in the seven cor-DEGs-DEPs genes (Fig. 3). The KEGG pathway analysis results showed that three KEGG pathways were significantly enriched at both mRNA and protein levels (i.e., glyoxylate and dicarboxylate metabolism, base excision repair and nitrogen metabolism) and three were significantly enriched at the mRNA level (i.e., arginine biosynthesis, alanine, aspartate and glutamate metabolism, and carbon fixation in photosynthetic organisms).

### Confirmation of qRT-PCR

In order to evaluate the transcriptome sequencing data, 10 of the cor-DEGs-DEPs genes were selected for RT-PCR. The relative expression levels of the 10 genes are shown in Fig. 4. Differential gene expression identified using real-time quantification was the same as that identified using RNA-seq. Although the expression of some genes was slightly different, the same general trend was observed (Fig. 5). Therefore, the transcriptome sequencing results were considered reliable.

## Discussion

In an organism, the transcriptome is the intermediate form of gene expression and the proteome is the final form of gene expression. Because gene expression is regulated at different levels, traditional transcription level studies cannot fully reveal the abundance of a protein [23], therefore, it is more important to study the proteome on the basis of the transcriptome to reveal the related mechanism. In this study, comparisons of transcriptomes of seedlings grown under different conditions suggested that the AC_N vs EC_N comparison had the greatest number of DEGs, whereas AC_hN vs EC_hN had the greatest number of DEPs.On the one hand, an explanation for this result may be that the biological processes of the transcriptome and proteome are not equal in nature, and that expression of some transcripts/genes does not result in protein product expression. On the other hand, it may be that post-transcriptional modification, post-translational modification, and protein degradation affect the amount of protein, and/or; it may reflect different detection technologies, gene detection technology maturity and protein detection technology [24].Inconsistencies between genes and their corresponding proteins have also been reported in another study [25].

### Effect of different $CO_2$ concentrations and nitrogen supply on P. bournei photosynthesis

Complexes that bind to the thylakoid membrane include the light system reaction center complex (RC), the light-harvesting pigment–protein complex (LHC), the cytochrome b6/f complex (cyt-b6/f) and the ATP synthase (ATPase) [26].Chlorophyll and other pigment–protein complexes are present in the RC and LHC. Plant photosynthetic pigment–protein complexes are key factors in the photoreaction [27]. Cyt-b6/f is an intermediate electron transport system that binds to both light systems [27]. ATPase is a key enzyme in photophosphorylation and catalyzes the synthesis of ATP [28]. Our analyses showed that the expression of genes and proteins involved in the light reaction of *P. bournei* seedlings treated with medium nitrate under $eCO_2$ was lower than that under $aCO_2$. These genes are responsible for coding LHC, RC, Cyt-b6/f, and ATPase in the transcriptome and the proteins included ATPase, ferredoxin and photosystem I subunit in the proteome. The expression of these genes or proteins was not significantly changed or upregulated in seedlings treated with high nitrate or ammonium under $eCO_2$, which suggests that the photosynthesis of *P. bournei* seedlings could be regulated by changing the nitrogen supply and form under an $eCO_2$ concentration by controlling light energy absorption, transformation, electron transfer and photophosphorylation. Studies by Haruhiko et al. [29] and Xu [30] have also shown that growing plants under $eCO_2$ conditions has an obvious effect on the plant light reaction.

### Glyoxylate and dicarboxylate metabolism of P. bournei affects the regulation of photosynthesis by nitrogen under $eCO_2$

Glyoxylate is an important metabolite of photorespiration and one of the important substances regulating photorespiration [31]. In the glyoxylate cycle, isocitric acid is catalyzed by isocitric acid lyase and malate synthase to form large amounts of succinate and malate [27]. Malate dehydrogenase (MDH) catalyzes the reversible conversion between malate and oxalacetic acid and is involved in many important metabolic pathways such as the tricarboxylic acid cycle (TCA cycle), glyoxylate cycle, malate-compartment shuttle and $CO_2$ fixation in photosynthesis [32]. The results showed that the specific genes and proteins enriched in the glyoxylate and dicarboxylate pathway of *P. bournei* included *MDH2* encoding MDH, which suggestted that MDH played a role in the regulation of photosynthesis by nitrogen in response to elevated $CO_2$. On the one hand, it might be that the supply of a different form of nitrogen affects $CO_2$ fixation in chloroplasts by affecting the expression of the *MDH2* gene. On the other hand, it was also possible that the expression of the *MDH2* gene affects the photorespiration of plants, which in turn affects the absorption of nitrate, which affects the photosynthetic efficiency.

### Galactose and nitrogen metabolism of P. bournei are involved in the regulation of photosynthesis by nitrogen under $eCO_2$

Inositol 3-alpha-galactosyltransferase (Gols) is the key enzyme involved in raffinose synthesis in galactose metabolism and a key gene in plants for environmental stress tolerance [33]. Hexokinase (HK) regulates sugar metabolism in plants and is one of the key enzymes in the glycolytic process [34]. Our

results showed that the expression of GolS and HK involved in galactose metabolism in *P. bournei* seedlings treated with a moderate application of nitrate decreased under $eCO_2$; however, the downregulated expression of related genes was alleviated by increasing the application of nitrate or ammonium. The increase of nitrate or ammonium adjusted the sugar metabolism of *P. bournei* seedlings under $eCO_2$. NADH, an electron donor reduced by nitrate in roots, is derived from glycolysis [27]. As a result, $eCO_2$ affects the energy supply of plants on the one hand and nitrate reduction in roots on the other hand.

Nitrogen metabolism is one of the most basic forms of metabolism in plants and affects many other physiological functions of plants [35]. Our results showed that the expression of genes related to nitrogen metabolism in *P. bournei* seedlings treated with a moderate application of nitrate was significantly decreased under $eCO_2$. However, the expression of genes encoding nitrate reductase, nitrite reductase, and glutamine synthetase (i.e., *NR*, *nirA*, and *glnA*, respectively) did not change significantly in seedlings treated with a high application of nitrate or a moderate application of ammonium. Our results showed that the nitrogen metabolism of *P. bournei* seedlings was adversely affected by applying a moderate amount of nitrate under $eCO_2$ but that this could be alleviated by changing the supply of nitrogen, which explains the differences in photosynthesis and the final growth performance of *P. bournei* seedlings under different nitrogen supplies and $CO_2$ concentrations. These findings support those of Buchner et al. [36], who found that $eCO_2$ affected the expression of genes involved in nitrate reduction.

### glnA and rbcS are associated with the effects of $eCO_2$ and nitrogen on photosynthesis

KEGG enrichment analyses of cor-DEGs-DEPs genes showed that two cor-DEGs-DEPs genes,*glnA* and *rbcS*, which affect nitrogen assimilation and photosynthesis, respectively, were significantly enriched in the nitrogen metabolic and glyoxylate and dicarboxylate metabolic pathways. We suggest that the transcription and protein levels of glnA and rbcS in *P. bournei* seedlings affect the response of photosynthesis to $eCO_2$ and the regulation of photosynthesis by nitrogen. Under $eCO_2$, plant photosynthesis may be downregulated. The reason for this is thought to be due to the downregulation of the gene encoding Rubisco [37, 38], a key enzyme in plant photosynthesis. It has also been suggested that a decrease in the nitrogen level causes photosynthesis to decline [39, 40]. In this study, we showed that the expression of *glnA* and *rbcS* decreased significantly at the transcript and protein level in seedlings treated with a moderate application of nitrate under $eCO_2$. This suggests that the synthesis of key photosynthetic enzymes and nitrogen absorption were affected under $eCO_2$ conditions, leading to the decline of photosynthesis. The expression of glnA and rbcS either did not change or was upregulated at the transcript and protein level in *P. bournei* seedlings treated with a high level of nitrate or a moderate level of ammonium under $eCO_2$. This suggests that the adverse effects of $eCO_2$ on the synthesis of key photosynthetic enzymes and nitrogen absorption in *P. bournei* seedlings were alleviated and, therefore, the downregulation of photosynthesis was finally alleviated.

$CO_2$ from bundle sheath cells enters the Calvin cycle and is immobilized by Rubisco, a key enzyme in the carbon cycle that catalyzes the carboxylation and oxygenation of ribulose-1,5-bisphosphate and regulates the relationship between the two [41, 42]. The content and activity of Rubisco were significantly positively correlated with the photosynthetic rate [43]. The Rubisco protein is mainly controlled by the content of *rbcS* [44]. Some studies have shown that the expression of the *rbcS* gene was downregulated under $eCO_2$ [37, 38]. In this study, the expression of *rbcS* was downregulated in the AC_N vs EC_N comparison but was unchanged in AC_hN vs EC_hN and AC_A vs EC_A (Table 3),which suggests that different nitrogen forms and supply affected the photosynthesis of *P. bournei* seedlings by regulating the expression of *rbcS* under $eCO_2$.

Ammonium absorbed from soil or reduced by nitrate is assimilated to amino acids by ammonia assimilation; glutamine synthetase is the key enzyme of ammonia assimilation [27].In this study, the expression of *glnA* was downregulated in AC_N vs EC_N, upregulated in AC_hN vs EC_hN and unchanged in AC_A vs EC_A (Table 3). *glnA* may have been upregulated in the AC_hN vs EC_hN comparison because the high nitrate application promoted nitrogen metabolism, which improved the expression of *glnA* [45]. The expression of *glnA* was downregulated in the AC_N vs EC_N comparison but was unchanged in AC_A vs EC_A, which may reflect the effect of $eCO_2$ on the expression of *MDH2*. Under $eCO_2$, the expression of *MDH2* in the AC_N vs EC_N comparison was downregulated but was unchanged in AC_A vs EC_A. MDH catalyzes the reversible conversion between malate and oxaloacetic acid and is mainly involved in the metabolic pathways of the TCA cycle, photosynthesis, and so on [46]. Nitrate reduction in plant roots requires glycolysis to provide NADH: MDH is the key enzyme in glycolysis [27]. NADH formed in photorespiration can be transferred to the cytoplasm via the oxaloacetic acid-malate transporter, which needs MDH catalysis for nitrate reduction in leaves [47]. Downregulation of *MDH2* could affect glycolysis, photorespiration, and nitrate reduction. Furthermore, MDH is a key enzyme in the TCA cycle, which is a major source of energy for life [48]. The effect of $eCO_2$ on energy supply via the expression of *MDH2* may explain why high nitrate and ammonium alleviated the decline of photosynthesis in *P. bournei*.

## Conclusions

Out analyses of the transcriptome and proteome showed that $eCO_2$ affected not only photosynthesis but also the metabolism of glucose, nitrogen, glyoxylate and dicarboxylate in *P. bournei* seedlings, resulting in a decrease in the photosynthetic efficiency. However, nitrogen applied in the form of ammonium alleviated the effects of $eCO_2$ on related physiological processes. The expression of *glnA* and *rbcS* affected the photosynthetic response of *P. bournei* to $eCO_2$ and the regulation of photosynthesis by nitrogen at both the transcript and protein levels. This study strengthens our understanding of the mechanism of $eCO_2$ and the regulation of photosynthesis by nitrogen at the molecular level and provides a theoretical reference for the cultivation of *P. bournei* seedlings to cope with $eCO_2$ concentrations in the future.

## Methods

Materials and methods

We have previously described the plant materials and fertilizer applications used in this study [9]. In brief, in January 2019, one-year-old *P. bournei* container seedlings grown from seeds of the same mother plant (Rongjiang, Guizhou, longitude E108°30'59" , latitude N25°28'47") identified by Prof. Mingtai An (Guizhou University). The Rongjiang forest service provided permission to collect the samples of *P. bournei.* A voucher specimen of this material was deposited in the herbarium of Guizhou University Forestry College, No. XF20140728-087. The seedlings were selected and transplanted to pots containing 1.5 kg of yellow soil, with one seedling per pot. The soil nutrient content was as follows: total N, 0.84 $g \cdot kg^{-1}$; alkali N, 28.3 $mg \cdot kg^{-1}$; total phosphorus, 0.23 $g \cdot kg^{-1}$; available phosphorus, 7.8 $mg \cdot kg^{-1}$; total potassium, 21.6 $g \cdot kg^{-1}$; available potassium, 207.3 $mg \cdot kg^{-1}$. Treatments were applied four months after seedlings were transplanted to allow time for recovery. The N fertilizers applied in this experiment were calcium nitrate and ammonium sulfate, the phosphate fertilizer was superphosphate, and the potassium fertilizer was potassium chloride.

We have previously described theopen-top air chamber used to simulate $eCO_2$ conditions and the experimental treatments [9]. In brief, seedlings were treated with either an ambient $CO_2$($aCO_2$) concentration of 280–450 $\mu mol \cdot mol^{-1}$ or a controlled $eCO_2$ concentration of 700 $\mu mol \cdot mol^{-1}$, and with either a moderate level of nitrate ($NO_3^-$; 0.8 g per seedling), a high level of nitrate ($hNO_3^-$; 1.2 g per seedling), or a moderate level of ammonium ($NH_4^+$; 0.8g per seedling), i.e., six treatments in total. There were 45 replicates of each treatment and, therefore, 270 pots in total. The N applications were divided into three equal quantities and applied on June $3_{rd}$, July $3_{rd}$, and August $2_{nd}$. The $CO_2$ treatments began on June $12_{th}$ and ended on September $8_{th}$. Phosphorus and potassium were also applied to seedlings on June $3_{rd}$, July $3_{rd}$, and August $2_{nd}$. The phosphorus and potassium application rate was based on the moderate level of N application (i.e., $N:P_2O_5:K_2O$ = 1:1:1). The transcriptomic and proteomic profiles obtained when seedlings were grown under each of the treatments were assessed at the end of the $CO_2$ treatment.

### RNA extract and library preparation

Total RNA was extracted using Trizol reagent according to the manufacturer's protocol (Takara Bio Inc., Otsu, Japan). The total RNA was checked for quality and quantity using an Agilent 2100 bioanalyzer (Agilent Technologies, Santa Clara, CA, USA). The libraries were constructed using a TruSeq Stranded mRNA LTSample Prep Kit (Illumina, San Diego, CA, USA) according to the manufacturer's instructions. The Illumina HiSeq 2500 system was used to sequence the qualified cDNA libraries. Three biological replicates were used in the RNA-seq experiments involving each sample and were sequenced as separate libraries.

### RNA-sequencing data analysis

First, raw data (raw reads) were quality controlled using SeqPrep (https://github.com/jstjohn/SeqPrep) and Sickle (https://github.com/najoshi/sickle) software. The clean reads were assembled using Trinity (https://github.com/trinityrnaseq/trinityrnaseq). The clean reads for each sample were compared with a reference sequence obtained from the Trinity assembly to get the mapping result for each sample.

Raw counts were analyzed using the software DESeq2 and differentially expressed genes/transcripts among the three comparison groups were analyzed. The following default parameter was used to identify differentially expressed genes (DEGs): an adjusted *p*-value of <0.05 and a |log2 fold change (FC)|of ≥1. Kyoto Encyclopedia of Genes and Genomes (KEGG, www.kegg.jp/kegg/kegg1.html) pathway enrichment and Gene Ontology (GO, http://www.geneontology.org/) analysis of DEGs was performed using the Majorbio Bio-Pharm Technology Co. Ltd. cloud platform (Shanghai, China). The resulting P-values were adjusted using Benjamini and Hochberg·s approach for controlling the false discovery rate (FDR).

### Protein extraction, protein digestion and iTRAQ labeling

Seedling samples were collected, ground with liquid nitrogen, and protein lysate (8 M urea + 1% SDS) was added in a 1:5 ratio. The supernatant was centrifuged at 4°C for 30 min at 16,000 *g* before adding five volumes of pre-chilled acetone, followed by precipitation overnight at –20°C. After precipitation, the precipitate was centrifuged at 12,000 *g* at 4°C for 30 min to collect the precipitate. The precipitate was washed and air-dried with 90% pre-chilled acetone. The precipitate was dissolved using protein lysate (8 mM urea + 1% SDS) and then centrifuged to obtain the supernatant. Protein concentrations were quantified using a BCA Protein Assay Kit (Bio-Rad, USA) and SDS-PAGE.

Triethylammonium bicarbonate (TEAB) buffer followed by tris-(2-carboxyethyl) phosphine (TCEP) was added to a 100 μg protein sample to make a final TEAB concentration of 100 mM, and a final TCEP concentration of 100 mM. The reaction time was 60 min at 37°C. Then, iodoacetamide (IAM) was added to a final concentration of 40 mM; the dark reaction time was 40 min at room temperature. Pre-chilled acetone (acetone:sample v/v = 6:1) was added to each tube and precipitated at –20°C for 4 hours followed by centrifugation (10,000 *g*) for 20 minutes, and then precipitated. The sample was fully dissolved with 100 μl 100 mM TEAB. Trypsin was added at an enzyme:protein (w/w) ratio of 1:50 and then incubated at 37°C overnight to allow enzymolysis to take place.

After trypsin digestion, the peptide was removed using a vacuum pump and the polypeptide was dissolved in 0.5 M TEAB. The tryptic peptides were labeled using an iTRAQ reagent 8-plex kit (SCIEX, Foster City, CA, USA). The iTRAQ was centrifuged and isopropanol was added. A tube of iTRAQ was added for every 100 μg of polypeptide and then incubated at room temperature for 2 hours before adding 50 μl of ultrapure water.

### High pH RPLC separation and mass spectrometry analysis

The samples were fractionated by performing high pH reversed-phase liquid chromatography (RPLC, Acquity Ultra Performance LC, Waters, Milford, MA, USA). The collected fractions (20 fractions) were then pooled to form 10 fractions. Each fraction was concentrated by vacuum centrifugation. Next, a 4-μl sample of each fraction was injected into a Q-Exactive mass spectrometer that was coupled to an Easy-1200 (Thermo Fisher Scientific, Waltham, MA, USA) for LC-MS/MS analysis. Survey full-scans of MS spectra (m/z 350–1300) were acquired with a mass resolution of 70 K, followed by 20 sequential high-energy collisional dissociation MS/MS scans with a resolution of 17.5 K.

### Proteomic analysis and correlation analysis of transcriptome and proteome data

The threshold for differentially expressed proteins (DEPs) was set at a *p*-value of < 0.05 and an FC of >1.2 or <0.83. KEGG pathway and GO enrichment analysis of differentially expressed genes (DEGs) was performed on the cloud platform of Majorbio Bio-Pharm Technology Co. Ltd. (Shanghai, China). The resulting P-values were adjusted using Benjamini and Hochberg's approach for controlling the FDR. If a gene and its corresponding protein in a comparison were expressed, the gene and its corresponding protein were considered to be correlated. If a gene and its corresponding protein were significantly expressed in compared treatments, they were considered to be cor-DEGs-DEPs.

### qRT-PCR analysis

To verify the accuracy of the transcriptome results, 10 DEGs were selected and detected using real-time quantitative techniques. TUA was used as an internal reference (F: 5'–GATGCTTTCAACACCTTCTTCAG–3', R: 5'–GGCGAAGTTGTTGGCAGC–3'). Total RNA was subjected to reverse transcription using a SYBR Green PCR Master Mix (TaKaRa) kit with a gDNA Eraser (Perfect for Real Time). cDNA was synthesized using a 20 μl reaction system comprising template RNA, 10 μl; dT primer, 1 μl; random primer, 1 μl; reaction buffer, 4 μl; 10 mM dNTP mix, 2 μl; riboLock RNase inhibitor, 1 μl; and RevertAid M-MuLV RT, 1 μl. All primers used for qRT-PCR are listed in Additional file 7: Table S3. The reaction conditions were as follows: 42°C for 60 min and then 70°C for 5 min. Real-time PCR was performed using SYBRs PremixEx Taq II (TaKaRa) in an ABI StepOne™ Plus Real-Time PCR System (Roche, Switzerland). The real-time PCR reaction conditions were as follows: step 1, 95°C for 2 min; step 2, 40 cycles of 95°C for 5 s and 60°C for 30 s. The relative expression of each of the 10 genes was calculated using the $2^{-\Delta\Delta Ct}$ relative quantification method.

### Statistical analysis

All data were analyzed using the Statistical Product and Service Solutions (SPSS) version 23.0. Data were assessed for significant differences by performing Tukey's tests. Figures and tables were constructed using Microsoft Office 2007.

## Abbreviations

ATPase: ATP synthase; BP: biological process; CC: cellular component; cor-DEGs-DEPs: correlation-DEGs-DEPs; cyt-b6/f: cytochrome b6/f complex; DEGs: differentially expressed genes; DEPs: differentially expressed proteins; GO: Gene Ontology; GolS: Inositol 3-alpha-galactosyltransferase; HK: hexokinase; KEGG: Kyoto Encyclopedia of Genes and Genomes; LHC: light-harvesting pigment–protein complex; MDH: malate dehydrogenase; MF: molecular function; RC: center complex; RCA: rubisco activase; Rubisco: ribulose-1,5-bisphosphate carboxylase/oxygenase; TCA cycle: tricarboxylic acid cycle

## Declarations

### Ethics approval and consent to participate

All methods were carried out in accordance with relevant guidelines and regulations.

### Consent for publication

Not applicable.

### Availability of data and material

The data supporting the results of this article are included within the article and the provided supplementary files. All sequencing data are available through the NCBI Sequence Read Archive under the accession number PRJNA817391 (www.ncbi.nlm.nih.gov/search/all/?term=PRJNA817391). The mass spectrometry proteomics data have been deposited to the ProteomeXchange Consortium via the iProX partner repository with the dataset identifier PXD032683 (http://proteomecentral.proteomexchange.org/cgi/GetDataset?ID=PXD032683).

### Competing interests

The authors declare that they have no competing interests.

### Funding

This research was funded by the Guizhou Province Technology Plan Project, QianKe He Foundation (2019)1407 and Guizhou Province High-level Innovative Talents Training Plan Project (2016) 5661.

### Authors' contributions

XW and XLW conceived this study; XW and SQC carried out the experiments; XW, XLW and GYW analyzed the results; XW wrote the manuscript with input from the other authors. All authors have read and agreed to the published version of the manuscript.

### Acknowledgements

Not applicable.

## References


1. Reddy AR, Rasineni GK, Raghavendra AS. The impact of global elevated $CO_2$ concentration on photosynthesis and plant productivity. Curr Sci. 2010;99:46–57.
2. Roumet C, Garnier E, Suzor H, Salager JL, Roy J. Short and long-term responses of whole-plant gas exchange to elevated $CO_2$ in four herbaceous species. Environ Exp Bot. 2000;43:155–69.
3. Jach ME, Ceulemans R. Short- versus long-term effects of elevated $CO_2$ on night-time respiration of needles of Scots pine (*Pinus sylvestris* L.). Photosynthetica. 2000;38:57–67.
4. Erice G, Irigoyen JJ, Pérez P, Martínez-Carrasco R, Sánchez-Díaz M. Effect of elevated $CO_2$, temperature and drought on photosynthesis of nodulated alfalfa during a cutting regrowth cycle. Physiol Plant. 2010;126:458–68.
5. Seneweera S, Makino A, Mae T, Basra AS. Response of rice to p($CO_2$) enrichment: the relationship between photosynthesis and nitrogen metabolism. J Crop Improv. 2005;38:289–99.
6. Seneweer, S, Makino A, Hirotsu N, Norton R, Suzuki Y. New insight into photosynthetic acclimation to elevated $CO_2$: the role of leaf nitrogen and ribulose-1,5-bisphosphate carboxylase/oxygenase content in rice leaves. Environ Exp Bot. 2011;71:128–36.
7. Bryant J, Taylor G, Frehner M. Photosynthetic acclimation to elevated $CO_2$ is modified by source:sink balance in three component species of chalk grassland swards grown in a free air carbon dioxide enrichment (FACE) experiment. Plant Cell Environ. 2010;21:159–68.
8. Han WJ, Liao FY, He P. The photosynthetic response of *Phoebe bournei* to doubled $CO_2$ concentration in air. J Cent South Univ For Tech. 2003;23:62–5.
9. Wang X, Wei XL, Wu GY, Chen SQ. Effects of different nitrogen forms and supply on photosynthetic characteristics and growth of Phoebe bournei seedlings under elevated $CO_2$ concentration. Scientia Silvae Sinicae, 2021; 57,173–181.
10. Wang X, Wei XL, Wu GY, Chen SQ. High nitrate or ammonium applications alleviated photosynthetic decline of *Phoebe bournei* seedlings under elevated carbon dioxide. Forests. 2020;11:293.
11. Ray D, Sheshshayee MS, Mukhopadhyay K, Bindumadhava H, Prasad TG, Kumar MU. High nitrogen use efficiency in rice genotypes is associated with higher net photosynthetic rate at lower rubisco content. Biologia Plantarum, 2003;46:251–6.
12. Hazra S, Swain DK, Bhadoria PBS. Wheat grown under elevated $CO_2$ was more responsive to nitrogen fertilizer in Eastern India. Eur J Agron. 2019;105:1–12.
13. Rubio-Asensio, JS, Bloom, AJ. Inorganic nitrogen form: a major player in wheat and Arabidopsis responses to elevated $CO_2$. J Exp Bot. 2017;68:2611–25.
14. Wang H, Lan P, Shen RF. Integration of transcriptomic and proteomic analysis towards understanding the systems biology of root hairs. Proteomics. 2016;16:877–93.
15. Sun CQ, Chen FD, Teng NJ, Yao YM, Dai ZL. Transcriptomic and proteomic analysis reveals mechanisms of low pollen-pistil compatibility during water lily cross breeding. BMC Plant Biol. 2019;19:542.
16. Zhang XQ, Bai L, Sun HB, Yang C, Cai BY. Transcriptomic and proteomic analysis revealed the effect of funneliformis mosseae in soybean roots differential expression genes and proteins. J Proteome Res, 2020;19, 3631–3643.
17. Kumar S, Sreeharsha RV, Mudalkar S, Sarashetti PM, Reddy AR. Molecular insights into photosynthesis and carbohydrate metabolism in *Jatropha curcas* grown under elevated $CO_2$ using transcriptome sequencing and assembly. Sci Rep. 2017;*7*:11066.
18. Li P, Ainsworth EA, Leakey ADB, Ulanov A, Lozovaya V, Ort DR, Bohnert HJ. Arabidopsis transcript and metabolite profiles: ecotype-specific responses to open-air elevated $CO_2$. Plant Cell Environ. 2008;31,1673–87.
19. Fukayama H, Sugino M, Fukuda T, Masumoto C, Taniguchi Y, Okada M,Sameshima R, Hatanaka T, Misoo S, Hasegawa T, Miyao M. Gene expression profiling of rice grown in free air $CO_2$ enrichment (FACE) and elevated soil temperature. Field Crop Res. 2011;121:195–9.
20. Aranjuelo I, Cabrera-Bosquet L, Morcuende R, Avice JC, Nogués S, Araus JL, Martínez-Carrasco R, Pérez P. Does ear C sink strength contribute to overcoming photosynthetic acclimation of wheat plants exposed to elevated $CO_2$? J Exp Bot. 2011;62:3957–69.
21. Aranjuelo I, Sanz-Sáez Á, Jáuregui I, Irigoyen JJ, Araus JL, Sánchez-Díaz M, Erice G. Harvest index, a parameter conditioning responsiveness of wheat plants to elevated $CO_2$. J Exp Bot. 2013;64:1879–92.
22. Zhao X, Li WF, Wang Y, Ma ZH, Yang SJ, Zhou Q, Mao J, Chen BH. Elevated $CO_2$ concentration promotes photosynthesis of grape (*Vitis vinifera* l. cv. 'pinot noir') plantlet in vitro by regulating Rbcs and Rca revealed by proteomic and transcriptomic profiles. BMC Plant Biol. 2019;19:42.
23. Hack CJ. Integrated transcriptome and proteome data: the challenges ahead. Brief Funct Genomic Proteomic. 2004; 3:212–9.
24. Ji FS. Analysis of banana responses salt stress of transcriptome and proteome. Hainan University; 2017.
25. Du CF. Analysis of transcriptome and proteome induced by low temperature in *Brassica napus L*.Huazhong Agricultural University; 2016.
26. Staehelin L A, van der Staay G W M. Structure, composition, functional organization and dynamic properties of thylakoid membranes. In: Ort DR, Yocum CF, Heichel IF, editors. Oxygenic Photosynthesis: The Light Reactions. Advances in Photosynthesis and Respiration, vol 4, Dordrecht: Springer; 1996. p. 11–30.
27. Wang Z. Plant Physiology, China Agriculture Press; 2005.
28. Mathur S, Gupta AK. Histoenzymological study on the toxicity of copper sulphate in the digestive glands of *Lymnaea luteola*. J Environ Bio. 2008;29:201.
29. Haruhiko T, Akira N, Jun M, Taka-aki O. Light-intensity-dependent expression of Lhc gene family encoding light-harvesting chlorophyll-a/b proteins of photosystem II in *Chlamydomonas reinhardtii*. Plant Physiol. 2002;130:325–33.

30. Xu MY. Effects of elevated $CO_2$ on photosynthetic characteristics and molecular mechanism in *Deyeuxia angustifolia*. Northeast Agricultural University; 2015.
31. De FC Carvalho J, Madgwick PJ, Powers SJ, Keys AJ, Lea PJ, Parry MAJ. An engineered pathway for glyoxylate metabolism in tobacco plants aimed to avoid the release of ammonia in photorespiration. BMC Biotechnol. 2011;11:111.
32. Song P. Study on the specific modification and function of malate dehydrogenase coenzyme in *Escherichia coli*. Anhui Normal University; 2012.
33. Wang Y, Liu H, Wang S, Li H, Xin Q. Overexpression of a common wheat gene *GALACTINOL SYNTHASE3* enhances tolerance to zinc in *Arabidopsis* and rice through the modulation of reactive oxygen species production. Plant Mol Biol Rep. 2015;34:1–13.
34. Li Q, Chen K, Hong JY, Zhou T, Xu MQ, Hu QQ, Li HR. Regulation of sugar metabolism in apricots by hexokinase and fructokinase during drying process. Modern Food Science and Technology. 2017;33:64–70,51.
35. Blevins DG. An overview of nitrogen metabolism in higher plants. In: Poulton JE, Romeo JT, Conn EE, editors. Plant Nitrogen Metabolism. Recent Advances in Phytochemistry, vol 23. New York: Plenum Press; 1989. p. 1–41.
36. Buchner P, Tausz M, Ford R, Leo A, Fitzgerald GJ, Hawkesford MJ, Tausz-Posch S. Expression patterns of C- and N-metabolism related genes in wheat are changed during senescence under elevated $CO_2$ in dry-land agriculture. Plant Sci. 2015;236:239–49.
37. Takatani N, Ito T, Kiba T, Mori M, Miyamoto T, Maeda S-I, Omata T. Effects of high $CO_2$ on growth and metabolism of *Arabidopsis* seedlings during growth with a constantly limited supply of nitrogen. Plant Cell Physiol. 2014;55:281–92.
38. Vicente R, Pérez P, Martínez-Carrasco R, Usadel B, Kostadinova S, Morcuende R. Quantitative RT-PCR platform to measure transcript levels of C and N metabolism-related genes in durum wheat: transcript profiles in elevated $CO_2$ and high temperature at different levels of N supply. Plant Cell Physiol. 2015;56:1556–73.
39. Seneweera S. Effects of elevated $CO_2$ on plant growth and nutrient partitioning of rice (*Oryza sativa* L.) at rapid tillering and physiological maturity. J Plant Interact. 2011;6:35–42.
40. Bloom AJ, Asensio JSR, Randall L, Rachmilevitch S, Cousins AB, Carlisle EA. $CO_2$ enrichment inhibits shoot nitrate assimilation in C3 but not C4 plants and slows growth under nitrate in C3 plants. Ecology. 2012;93:355–67.
41. Lundqvist T, Schneider G. Crystal structure of activated ribulose-1,5-bisphosphate carboxylase complexed with its substrate, ribulose-1,5-bisphosphate. Biol Chem. 1991;266:12604–11.
42. Ashida H, Danchin A, Yokota A. Was photosynthetic Rubisco recruited by acquisitive evolution from rubisco-like proteins involved in sulfur metabolism?. Res Microbiol. 2005;156:611–8.
43. Spreiter RJ, Salvucci ME. Rubisco: structure, regulatory interactions, and possibilities for a better enzyme. Annu Rev Plant Biol. 2002;53:449–75.
44. Suzuki Y, Makino A. Availability of rubisco small subunit up-regulates the transcript levels of large subunit for stoichiometric assembly of its holoenzyme in rice. Plant Physiol. 2012;160:533–40.
45. Grover HL, Nair TVR, Abrol YP. Nitrogen metabolism of the upper three leaf blades of wheat at different soil nitrogen levels. Physiol Plant. 1978;42:287–92.
46. Miller SS, Driscoll B T, Gregerson RG, Gantt JS, Vance CP. Alfalfa malate dehydrogenase (MDH): molecular cloning and characterization of five different forms reveals a unique nodule-enhanced MDH. Plant J. 2010;15:173–84.
47. Yu RC, Li MQ, Fan YP. Study on the relationship between photoabsorption and nitrogen metabolism-effects of inhibitors and metabolites of photoinduction on the light induction of nitrate reductase. Scientia Agricultura Sinica. 2002;49–52.
48. Penny D. An interpretive review of the origin of life research. Biol Philos. 2005;20:633–71.

## Tables

Table 1
KEGG pathway enrichment analysis of DEGs in *Phoebe bournei* leaves affected by $eCO_2$ and nitrogen supply

| Pathway | Definition | Gene id | KO ID | KO name | AC_N_vs_EC_N | | AC_hN_vs_EC_hN | | AC_A_vs_EC |
|---|---|---|---|---|---|---|---|---|---|
| | | | | | Log2FC | *p* value | Log2FC | *p* value | Log2FC |
| Photosynthesis - antenna proteins | Light-harvesting complex I chlorophyll a/b binding protein | TRINITY_DN6072_c0_g1 | K08907 | LHCA1 | -1.438 | 1.96E-22 | 0.297 | 0.184 | 0.602 |
| | | TRINITY_DN1459_c1_g2 | K08908 | LHCA2 | -1.015 | 5.53E-07 | -0.024 | 0.928 | 0.613 |
| | | TRINITY_DN1459_c1_g1 | K08908 | LHCA2 | -1.288 | 2.78E-13 | 0.168 | 0.470 | 0.614 |
| | | TRINITY_DN2179_c0_g1 | K08909 | LHCA3 | -1.115 | 1.74E-10 | 1.033 | 1.34E-08 | 0.636 |
| | Light-harvesting complex II chlorophyll a/b binding protein | TRINITY_DN4374_c0_g1 | K08912 | LHCB1 | -1.898 | 7.99E-43 | 0.858 | 6.34E-05 | 0.969 |
| | | TRINITY_DN5377_c0_g2 | K08912 | LHCB1 | -7.129 | 5.26E-05 | -5.401 | 0.168 | 2.096 |
| | | TRINITY_DN5153_c0_g1 | K08913 | LHCB2 | -1.716 | 3.77E-26 | 0.547 | 0.063 | 0.365 |
| | | TRINITY_DN6807_c0_g1 | K08916 | LHCB5 | -1.740 | 5.23E-35 | 0.500 | 0.066 | 0.569 |
| Photosynthesis | Photosystem II oxygen-evolving enhancer protein 2 | TRINITY_DN4587_c0_g3 | K02717 | psbP | -1.206 | 2.53E-11 | 0.253 | 0.258 | 0.506 |
| | | TRINITY_DN8439_c0_g3 | K02717 | psbP | -1.242 | 3.28E-17 | 0.259 | 0.226 | 0.156 |
| | | TRINITY_DN27584_c0_g1 | K03541 | psbR | -1.128 | 5.30E-19 | 0.328 | 0.047 | 0.344 |
| | | TRINITY_DN17206_c1_g2 | K03541 | psbR | -1.039 | 1.59E-16 | 0.388 | 0.004 | 0.392 |
| | | TRINITY_DN12047_c0_g1 | K02721 | psbW | -1.183 | 1.62E-17 | 0.425 | 0.019 | 0.385 |
| | | TRINITY_DN7923_c0_g2 | K02723 | psbY | -1.246 | 4.69E-16 | 0.011 | 0.962 | -0.035 |
| | Photosystem I subunit IV | TRINITY_DN5464_c0_g1 | K02693 | psaE | -1.021 | 5.66E-14 | 0.068 | 0.702 | 0.031 |
| | | TRINITY_DN12180_c0_g2 | K08905 | psaG | -1.491 | 5.15E-29 | 0.077 | 0.751 | 0.477 |
| | | TRINITY_DN570_c1_g1 | K02699 | psaL | -1.076 | 2.16E-17 | 0.313 | 0.061 | 0.319 |
| | | TRINITY_DN73178_c0_g2 | K02701 | psaN | -1.837 | 2.30E-40 | 0.872 | 0.000 | 0.748 |
| | | TRINITY_DN2005_c0_g2 | K14332 | psaO | -1.861 | 1.29E-30 | 0.096 | 0.739 | 0.311 |
| | Cytochrome b6-f complex iron-sulfur subunit [EC:7.1.1.6] | TRINITY_DN7055_c0_g1 | K02636 | petC | -1.654 | 0.002 | 1.741 | 1.08E-05 | -0.535 |
| | Ferredoxin–$NADP^+$ reductase [EC:1.18.1.2] | TRINITY_DN5187_c1_g1 | K02641 | petH | -1.353 | 6.09E-06 | 0.431 | 0.141 | -0.168 |
| | F-type $H^+$-transporting ATPase subunit delta | TRINITY_DN6730_c0_g1 | K02113 | ATPF1D, atpH | -1.261 | 8.15E-11 | 0.537 | 0.024 | -0.424 |
| | F-type $H^+$-transporting ATPase subunit b | TRINITY_DN17068_c0_g1 | K02109 | ATPF0B, atpF | -1.856 | 0.005 | 0.481 | 0.273 | 0.727 |
| | Plastocyanin | TRINITY_DN9256_c0_g1 | K02638 | petE | -1.578 | 3.30E-20 | 0.399 | 0.100 | 0.591 |

Abbreviations: AC_N vs EC_N, seedlings grown under an $aCO_2$ concentration and a moderate level of nitrate ($NO_3^-$) versus an $eCO_2$ concentration and a mod level of nitrate; AC_hN vs EC_hN, seedlings grown under $aCO_2$ and a high level of nitrate ($hNO_3^-$) versus $eCO_2$ and $hNO_3^-$; AC_A vs EC_A,seedlings grown und $aCO_2$ and a moderate level of ammonium ($NH_4^+$) versus $eCO_2$ and $NH_4^+$; KO ID, KEGG Orthology identifier; log2FC, log2 fold change

| | | | | | | | | | | |
|---|---|---|---|---|---|---|---|---|---|---|
| Galactose metabolism | Aldose 1-epimerase [EC:5.1.3.3] | TRINITY_DN6461_c0_g1 | K01785 | galM, GALM | -1.336 | 3.44E-05 | -0.695 | 0.005 | 0.526 | ( |
| | Alpha-galactosidase [EC:3.2.1.22] | TRINITY_DN507_c0_g1 | K07407 | galA, rafA | -1.430 | 1.44E-14 | -1.371 | 0.025 | -0.532 | ( |
| | | TRINITY_DN22610_c0_g1 | K07407 | galA, rafA | -1.489 | 3.88E-21 | 1.131 | 2.58E-05 | 1.130 | ( |
| | | TRINITY_DN4076_c0_g1 | K07407 | galA, rafA | -1.889 | 4.62E-31 | -0.503 | 0.045 | -0.196 | ( |
| | UDP-glucose 4-epimerase [EC:5.1.3.2] | TRINITY_DN41314_c0_g1 | K01784 | galE, GALE | -7.161 | 3.86E-05 | -4.840 | 0.049 | 5.269 | ( |
| | Inositol 3-alpha-galactosyltransferase [EC:2.4.1.123] | TRINITY_DN3723_c6_g1 | K18819 | GOLS | -1.708 | 3.75E-40 | 1.048 | 5.57E-06 | 0.906 | ( |
| | | TRINITY_DN3174_c11_g1 | K18819 | GOLS | -1.778 | 1.01E-43 | 1.074 | 1.59E-06 | 0.974 | 1 ( |
| | | TRINITY_DN4634_c1_g1 | K18819 | GOLS | 3.952 | 0.002 | 0.519 | 0.647 | -0.014 | ( |
| | | TRINITY_DN4634_c2_g1 | K18819 | GOLS | 1.367 | 5.03E-06 | 0.067 | 0.790 | 0.072 | ( |
| | Hexokinase [EC:2.7.1.1] | TRINITY_DN6200_c0_g3 | K00844 | HK | -1.004 | 1.66E-12 | 0.084 | 0.647 | 0.367 | ( |
| | Raffinose synthase [EC:2.4.1.82] | TRINITY_DN60249_c0_g1 | K06617 | E2.4.1.82 | 1.143 | 4.23E-07 | 0.208 | 0.439 | -0.083 | ( |
| | Alpha-glucosidase [EC:3.2.1.20] | TRINITY_DN6779_c0_g1 | K01187 | malZ | -2.103 | 0.001 | -0.019 | 0.972 | -0.135 | ( |
| | | TRINITY_DN3546_c0_g1 | K01187 | malZ | -2.071 | 2.16E-06 | 0.152 | 0.726 | 0.240 | ( |
| | 6-phosphofructokinase 1 [EC:2.7.1.11] | TRINITY_DN2052_c0_g4 | K00850 | pfkA, PFK | 1.356 | 2.09E-11 | -0.053 | 0.819 | 0.320 | ( |
| | | TRINITY_DN51643_c0_g1 | K00850 | pfkA, PFK | -1.554 | 0.001 | 0.185 | 0.691 | 0.579 | ( |
| Nitrogen metabolism | Nitrate reductase (NAD(P)H) [EC:1.7.1.1 1.7.1.2 1.7.1.3] | TRINITY_DN13282_c0_g1 | K10534 | NR | -2.624 | 7.67E-07 | 1.839 | 0.000 | 1.868 | ( |
| | Ferredoxin-nitrite reductase [EC:1.7.7.1] | TRINITY_DN45638_c1_g1 | K00366 | nirA | -2.053 | 1.55E-16 | 0.821 | 0.012 | 0.983 | ( |
| | Carbonic anhydrase [EC:4.2.1.1] | TRINITY_DN14769_c3_g1 | K01673 | cynT, can | -1.316 | 1.17E-17 | 0.086 | 0.720 | -0.256 | ( |
| | Cyanate lyase [EC:4.2.1.104] | TRINITY_DN4889_c0_g1 | K01725 | cynS | -2.347 | 2.00E-49 | -0.041 | 0.883 | 0.647 | ( |
| | Glutamate synthase (NADH) [EC:1.4.1.14] | TRINITY_DN21018_c0_g2 | K00264 | GLT1 | -1.284 | 0.004 | 0.069 | 0.800 | 1.098 | ( |
| | Glutamine synthetase [EC:6.3.1.2] | TRINITY_DN2115_c0_g1 | K01915 | glnA, GLUL | -2.878 | 3.80E-29 | -0.971 | 0.040 | 1.277 | ( |
| | | TRINITY_DN378_c2_g1 | K01915 | glnA, GLUL | -1.043 | 2.38E-07 | 1.085 | 1.96E-06 | 0.404 | ( |
| Glyoxylate and dicarboxylate metabolism | Acetyl-CoA C-acetyltransferase [EC:2.3.1.9] | TRINITY_DN14251_c0_g1 | K00626 | atoB | -3.836 | 8.52E-07 | -1.133 | 0.283 | 1.333 | ( |
| | | TRINITY_DN8905_c0_g1 | K00626 | atoB | -1.496 | 1.43E-05 | -0.018 | 0.958 | 0.963 | ( |
| | Malate dehydrogenase [EC:1.1.1.37] | TRINITY_DN7702_c0_g1 | K00026 | MDH2 | -1.116 | 3.50E-08 | -0.497 | 0.028 | 0.573 | ( |
| | (S)-2-hydroxy-acid oxidase [EC:1.1.3.15] | TRINITY_DN15870_c0_g1 | K11517 | HAO | -1.012 | 1.68E-13 | 0.331 | 0.117 | 0.222 | ( |
| | Phosphoglycolate phosphatase [EC:3.1.3.18 3.1.3.48] | TRINITY_DN14585_c0_g2 | K19269 | PGP, PGLP | -1.196 | 0.001 | 0.322 | 0.181 | 0.474 | ( |

Abbreviations: AC_N vs EC_N, seedlings grown under an $aCO_2$ concentration and a moderate level of nitrate ($NO_3^-$) versus an $eCO_2$ concentration and a mod level of nitrate; AC_hN vs EC_hN, seedlings grown under $aCO_2$ and a high level of nitrate ($hNO_3^-$) versus $eCO_2$ and $hNO_3^-$; AC_A vs EC_A,seedlings grown und $aCO_2$ and a moderate level of ammonium ($NH_4^+$) versus $eCO_2$ and $NH_4^+$; KO ID, KEGG Orthology identifier; log2FC, log2 fold change

| | | | | | | | | | |
|---|---|---|---|---|---|---|---|---|---|
| Ribulose-bisphosphate carboxylase small chain [EC:4.1.1.39] | TRINITY_DN4950_c1_g2 | K01602 | rbcS | -1.554 | 2.44E-29 | 0.734 | 0.001 | 0.703 | 7 |
| | TRINITY_DN69326_c0_g1 | K01602 | rbcS | -2.077 | 8.18E-07 | 2.172 | 4.39E-10 | -0.159 | |
| | TRINITY_DN54792_c0_g1 | K01602 | rbcS | -1.444 | 5.04E-12 | 2.653 | 3.27E-15 | -0.228 | |
| Glutamine synthetase [EC:6.3.1.2] | TRINITY_DN2115_c0_g1 | K01915 | glnA, GLUL | -2.878 | 3.80E-29 | -0.971 | 0.040 | 1.277 | |
| | TRINITY_DN378_c2_g1 | K01915 | glnA, GLUL | -1.043 | 2.38E-07 | 1.085 | 1.96E-06 | 0.404 | |
| Dihydrolipoamide dehydrogenase [EC:1.8.1.4] | TRINITY_DN808_c0_g1 | K00382 | DLD, lpd, pdhD | -1.034 | 7.78E-13 | 0.044 | 0.841 | 0.624 | |
| Glycine cleavage system H protein | TRINITY_DN9168_c0_g1 | K02437 | gcvH, GCSH | -1.247 | 0.001 | -0.234 | 0.430 | 0.821 | |
| | TRINITY_DN9168_c0_g3 | K02437 | gcvH, GCSH | 4.152 | 0.000 | 0.612 | 0.229 | -0.278 | |
| Formate dehydrogenase [EC:1.17.1.9] | TRINITY_DN17215_c0_g1 | K00122 | FDH | 2.855 | 0.003 | -2.737 | 0.018 | -1.432 | |
| Alanine-glyoxylate transaminase / Serine-glyoxylate transaminase / serine-pyruvate transaminase [EC:2.6.1.44 2.6.1.45 2.6.1.51] | TRINITY_DN57333_c0_g1 | K00830 | AGXT | -1.393 | 8.53E-11 | 0.772 | 0.006 | -0.419 | |

Abbreviations: AC_N vs EC_N, seedlings grown under an $aCO_2$ concentration and a moderate level of nitrate ($NO_3^-$) versus an $eCO_2$ concentration and a mod level of nitrate; AC_hN vs EC_hN, seedlings grown under $aCO_2$ and a high level of nitrate ($hNO_3^-$) versus $eCO_2$ and $hNO_3^-$; AC_A vs EC_A,seedlings grown und $aCO_2$ and a moderate level of ammonium ($NH_4^+$) versus $eCO_2$ and $NH_4^+$; KO ID, KEGG Orthology identifier; log2FC, log2 fold change

Table 2
KEGG pathway enrichment analysis of DEPs in *Phoebe bournei* leaves affected by $eCO_2$ and nitrogen supply

| Pathway definition | Definition | Accession | KO ID | KO name | AC_N_vs_EC_N | | AC_hN_vs_EC_hN | | AC |
|---|---|---|---|---|---|---|---|---|---|
| | | | | | FC | *p* value | FC | *p* value | FC |
| Glyoxylate and dicarboxylate metabolism | Malate dehydrogenase [EC:1.1.1.37] | TRINITY_DN11104_c0_g1_i1_orf1 | K00026 | MDH2 | 0.7706 | 0.0071 | 1.0208 | 0.2547 | 1.0 |
| | Glutamine synthetase [EC:6.3.1.2] | TRINITY_DN378_c2_g1_i2_orf1 | K01915 | glnA, GLUL | 0.7706 | 0.0175 | 1.2294 | 0.0006 | 1.0 |
| | | TRINITY_DN11240_c0_g1_i1_orf1 | | | 0.7849 | 0.0341 | 1.3175 | 0.0369 | 1.1 |
| | Alanine–glyoxylate transaminase / serine–glyoxylate transaminase / serine–pyruvate transaminase [EC:2.6.1.44 2.6.1.45 2.6.1.51] | TRINITY_DN1287_c0_g1_i1_orf1 | K00830 | AGXT | 0.8189 | 0.0118 | 0.9672 | 0.3323 | 1.0 |
| | | TRINITY_DN1287_c0_g1_i6_orf1 | | | 0.7928 | 0.0017 | 0.9603 | 0.1379 | 1.0 |
| | Formamidase [EC:3.5.1.49] | TRINITY_DN1537_c0_g1_i7_orf1 | K01455 | E3.5.1.49 | 1.2172 | 0.0054 | 1.0234 | 0.5274 | 0.7 |
| | Malate dehydrogenase [EC:1.1.1.37] | TRINITY_DN2183_c0_g2_i2_orf1 | K00025 | MDH1 | 1.2061 | 0.0219 | 0.9014 | 0.2649 | 0.8 |
| | Glutamate–glyoxylate aminotransferase [EC:2.6.1.4 2.6.1.2 2.6.1.44] | TRINITY_DN263_c0_g1_i10_orf1 | K14272 | GGAT | 0.7295 | 0.0089 | 1.1269 | 0.0203 | 1.0 |
| | | TRINITY_DN263_c0_g1_i6_orf1 | | | 0.7639 | 0.0045 | 1.0931 | 0.0846 | 1.0 |
| | Citrate synthase [EC:2.3.3.1] | TRINITY_DN474_c0_g2_i2_orf1 | K01647 | CS, gltA | 0.7976 | 0.0349 | 1.0100 | 0.9026 | 1.1 |
| | Ribulose-bisphosphate carboxylase small chain [EC:4.1.1.39] | TRINITY_DN4950_c1_g2_i2_orf1 | K01602 | rbcS | 0.6734 | 0.0195 | 0.9893 | 0.9328 | 1.0 |
| | Catalase [EC:1.11.1.6] | TRINITY_DN6014_c0_g1_i3_orf1 | K03781 | katE, CAT, catB, srpA | 0.8119 | 0.0360 | 1.3462 | 0.0012 | 1.2 |
| | Glyoxylate/hydroxypyruvate reductase [EC:1.1.1.79 1.1.1.81] | TRINITY_DN7326_c0_g1_i3_orf1 | K15919 | HPR2 | 0.8239 | 0.0024 | 1.0637 | 0.4065 | 1.0 |
| | Glycine hydroxymethyltransferase [EC:2.1.2.1] | TRINITY_DN8343_c0_g1_i4_orf1 | K00600 | glyA, SHMT | 0.7714 | 0.0184 | 0.9197 | 0.2346 | 0.9 |
| | Glycerate dehydrogenase [EC:1.1.1.29] | TRINITY_DN8601_c0_g1_i5_orf1 | K15893 | HPR1 | 0.7498 | 0.0343 | 0.9851 | 0.5639 | 0.9 |
| Photosynthesis | Photosystem I subunit VI | TRINITY_DN1063_c0_g1_i10_orf1 | K02695 | psaH | 0.7819 | 0.0218 | 1.0254 | 0.7947 | 1.1 |
| | Photosystem I subunit II | TRINITY_DN12085_c0_g1_i1_orf1 | K02692 | psaD | 1.3020 | 0.0255 | 0.8768 | 0.3100 | 1.3 |
| | F-type $H^+$-transporting ATPase subunit b | TRINITY_DN304_c2_g1_i2_orf1 | K02109 | ATPF0B, atpF | 0.7598 | 0.0097 | 1.0760 | 0.4989 | 1.2 |
| | F-type $H^+$-transporting ATPase subunit delta | TRINITY_DN9472_c0_g1_i7_orf1 | K02113 | ATPF1D, atpH | 0.6699 | 0.0222 | 1.1138 | 0.3970 | 1.0 |
| | ferredoxin | TRINITY_DN5630_c0_g1_i2_orf1 | K02639 | petF | 1.7843 | 0.0077 | 0.9047 | 0.1184 | 0.8 |
| | Photosystem II oxygen-evolving enhancer protein 1 | TRINITY_DN6231_c0_g1_i1_orf1 | K02716 | psbO | 1.3287 | 0.0047 | 0.9076 | 0.0326 | 0.8 |

Abbreviations: AC_N vs EC_N, seedlings grown under an $aCO_2$ concentration and a moderate level of nitrate ($NO_3^-$) versus an $eCO_2$ concentration and a mod nitrate; AC_hN vs EC_hN, seedlings grown under $aCO_2$ and a high level of nitrate ($hNO_3^-$) versus $eCO_2$ and $hNO_3^-$; AC_A vs EC_A,seedlings grown under $aCO_2$ moderate level of ammonium ($NH_4^+$) versus $eCO_2$ and $NH_4^+$; FC, fold change; KO ID, KEGG Orthology identifier

Table 3
KEGG pathway enrichment analysis of Cor-DEGs-DEPs genes in *Phoebe bournei* leaves affected by $eCO_2$ and nitroger

| Gene/protein accession | EC_N vs AC_N | | | | EC_hN vs AC_hN | | | | EC_A vs AC_A | | |
|---|---|---|---|---|---|---|---|---|---|---|---|
| | Gene | | Protein | | Gene | | Protein | | Gene | | Protein |
| | Log2FC | *p* value | FC | *p* value | Log2FC | *p* value | FC | *p* value | Log2FC | *p* value | FC |
| TRINITY_DN10641_c1_g1/ TRINITY_DN10641_c1_g1_i1_orf1 | -1.3286 | 3.341E-22 | 0.5821 | 0.0013 | 0.5759 | 0.0027 | 1.5513 | 0.0012 | 0.7772 | 4.071E-05 | 0.8539 |
| TRINITY_DN19829_c0_g1/ TRINITY_DN19829_c0_g1_i1_orf1 | 1.9167 | 1.751E-05 | 1.2575 | 0.0074 | 0.2091 | 0.5904 | 1.0183 | 0.7152 | -0.3182 | 0.6464 | 1.1223 |
| TRINITY_DN20438_c0_g1/ TRINITY_DN20438_c0_g1_i1_orf1 | -1.6665 | 2.243E-05 | 0.7434 | 0.0148 | 0.1429 | 0.6194 | 1.5476 | 0.2848 | 1.2097 | 0.0016 | 1.1478 |
| TRINITY_DN31503_c0_g2/ TRINITY_DN31503_c0_g2_i2_orf1 | -1.3346 | 0.0004 | 0.8106 | 0.0127 | 0.7439 | 0.0126 | 1.1080 | 0.3535 | -0.1006 | 0.8486 | 1.3426 |
| TRINITY_DN34301_c0_g1/ TRINITY_DN34301_c0_g1_i13_orf1 | -1.8906 | 1.758E-07 | 0.7972 | 0.0061 | 0.1082 | 0.7348 | 0.8012 | 0.0095 | 0.8616 | 0.0375 | 1.5747 |
| TRINITY_DN378_c2_g1/ TRINITY_DN378_c2_g1_i2_orf1 | -1.0430 | 2.377E-07 | 0.7706 | 0.0175 | 1.0855 | 1.96E-06 | 1.2294 | 0.0006 | 0.4042 | 0.1019 | 1.0790 |
| TRINITY_DN4950_c1_g2/ TRINITY_DN4950_c1_g2_i2_orf1 | -1.5541 | 2.443E-29 | 0.6734 | 0.0195 | 0.7338 | 0.0012 | 0.9893 | 0.9328 | 0.7027 | 0.0001 | 1.0636 |

Abbreviations: AC_N vs EC_N, seedlings grown under an $aCO_2$ concentration and a moderate level of nitrate ($NO_3^-$) versus an $eCO_2$ concentration and a moc seedlings grown under $aCO_2$ and a high level of nitrate ($hNO_3^-$) versus $eCO_2$ and $hNO_3^-$; AC_A vs EC_A,seedlings grown under $aCO_2$ and a moderate level of ID, KEGG Orthology identifier; log2FC, log2 fold change

## Figures

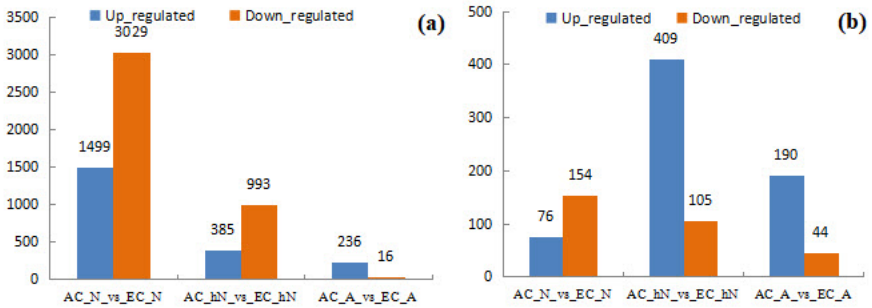



**Figure 1**

Number of differentially expressed transcripts and proteins obtained in response to elevated $CO_2$ and different nitrogen applications. **a.** Differentially expressed transcripts. **b.** Differentially expressed proteins. AC_N vs EC_N, *Phoebe bournei* seedlings grown under an $aCO_2$ concentration and a moderate level of nitrate ($NO_3^-$) versus an $eCO_2$ concentration and a moderate level of nitrate; AC_hN vs EC_hN, seedlings grown under $aCO_2$ and a high level of nitrate ($hNO_3^-$) versus $eCO_2$ and $hNO_3^-$; AC_A vs EC_A,seedlings grown under $aCO_2$ and a moderate level of ammonium ($NH_4^+$) versus $eCO_2$ and $NH_4^+$

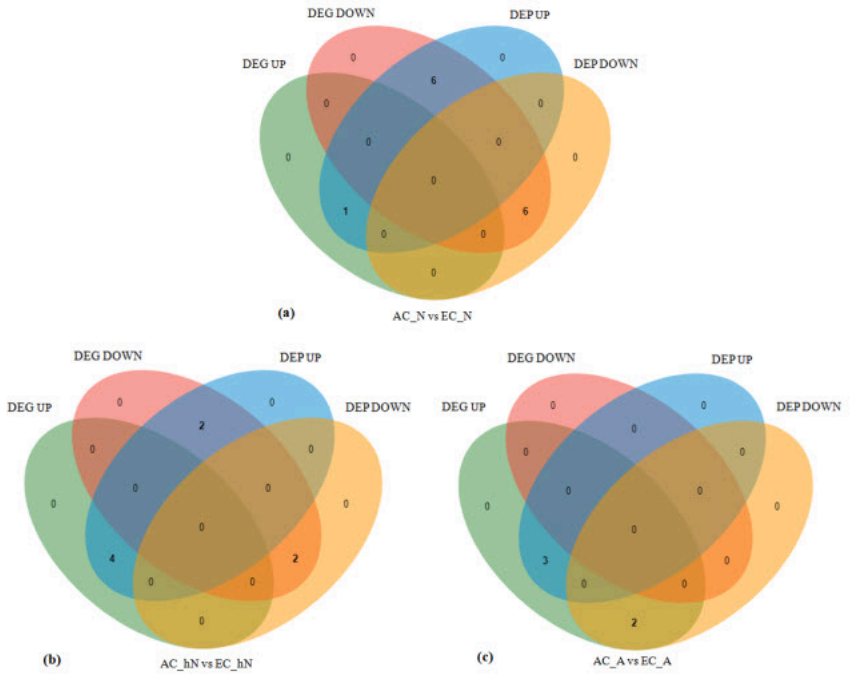



**Figure 2**

Venn diagram showing correlations between DEGs and the corresponding DEPs. Abbreviations: AC_N vs EC_N (a), *Phoebe bournei* seedlings grown under an $aCO_2$ concentration and a moderate level of nitrate ($NO_3^-$) versus an $eCO_2$ concentration and a moderate level of nitrate; AC_hN vs EC_hN (b), seedlings grown under $aCO_2$ and a high level of nitrate ($hNO_3^-$) versus $eCO_2$ and $hNO_3^-$; AC_A vs EC_A (c),seedlings grown under $aCO_2$ and a moderate level of ammonium ($NH_4^+$) versus $eCO_2$ and $NH_4^+$; DEG UP, number of differentially expressed genes upregulated; DEG DOWN, number of differentially expressed genes downregulated; DEP UP, number of differentially expressed proteins upregulated; DEP DOWN, number of differentially expressed proteins downregulated

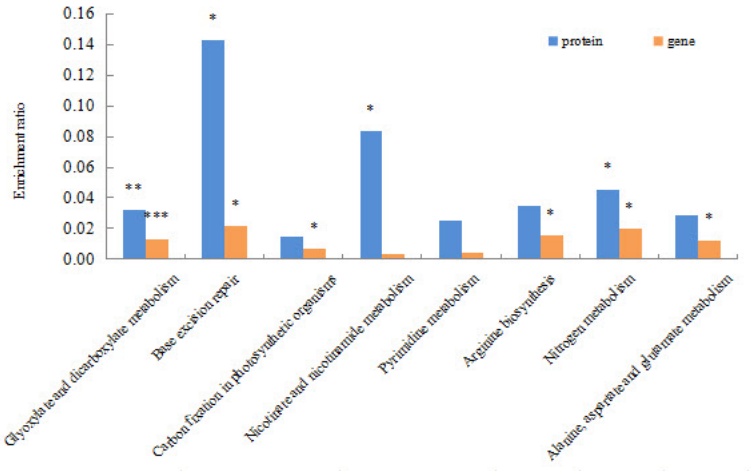



**Figure 3**

KEGG enrichment analyses of cor-DEGs-DEPs genes. Enrichment rate, the ratio of the number of proteins or genes enriched in the pathway to the number of proteins or genes annotated in the pathway. ***, $p<0.001$; **, $p<0.01$; *, $p<0.05$

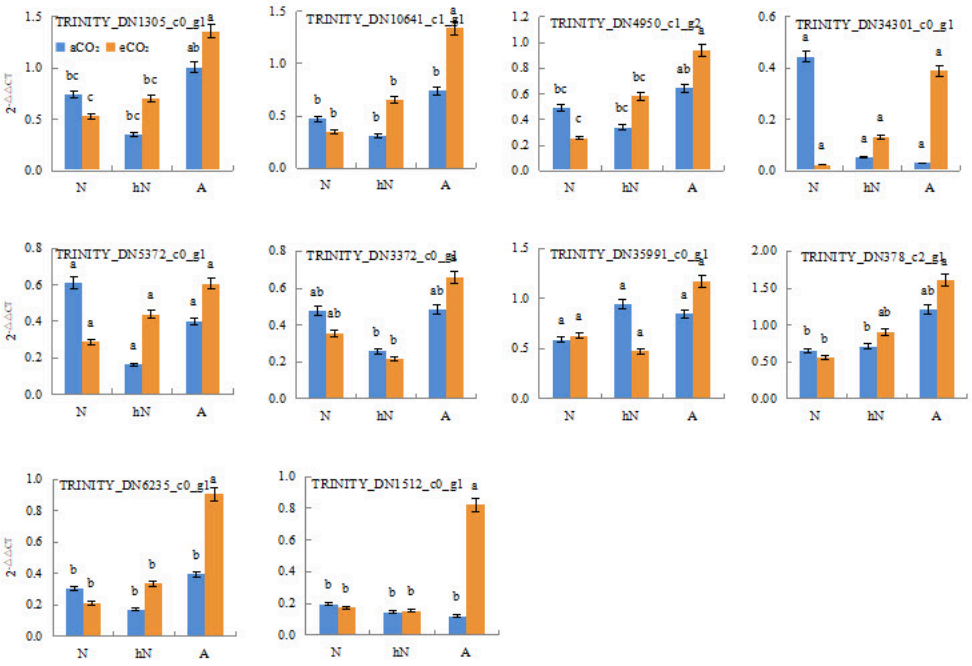



**Figure 4**

RT-PCR evaluation of the Relative expression of 10 cor-DEGs-DEPs genes identified in *Phoebe bournei* seedlings. Seedlings were grown under elevated and ambient $CO_2$ concentrations and applied with: N, a moderate level of nitrate; hN, a high level of nitrate; A, a moderate level of ammonium. Data shown are means ± the standard deviation. Different lowercase letters above the bars indicate a significant difference in the relative expression of a gene under different treatment conditions.

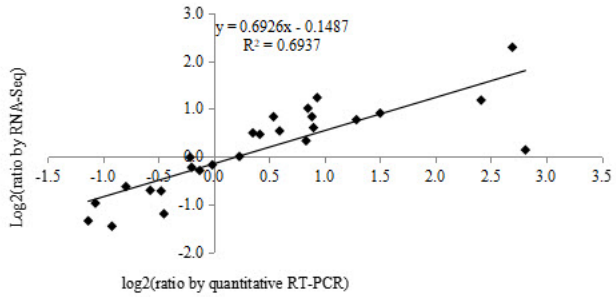



**Figure 5**

Correlation between RNA-seq and quantitative real-time PCR (qRT-PCR). Comparison of the log2 fold change of 10 DEGs identified by RNA-seq and qRT-PCR

## Supplementary Files

This is a list of supplementary files associated with this preprint. Click to download.

- Additionalfile1FigureS1GOanalysisforDEGs.docx
- Additionalfile2FigureS2GOanalysisforDEPs.docx
- Additionalfile3TableS1KEGGpathwayanalysisforDEGs.xls
- Additionalfile4TableS2KEGGpathwayanalysisforDEPs.xls
- Additionalfile5FigureS3ClusteranalysisofexpressionpatternsintheassociatedDEGs.png
- Additionalfile6FigureS4ClusteranalysisofexpressionpatternsintheassociatedDEPs.png
- Additionalfile7TableS3PrimerusedinthisstudyforqRTPCR.xlsx
- Supplementaryfileslegends.docx